Journal of Thermal Analysis and Calorimetry, Vol. 57 (1999) 447-458

EXCESS HEAT CAPACITY IN YTTRIA STABILIZED ZIRCONIA

T. Tojo[1], *T. Atake*[1*], *T. Mori*[2] *and H. Yamamura*[3]

[1]Materials and Structures Laboratory, Tokyo Institute of Technology, Nagatsuta-cho Midori-ku, Yokohama, 226-8503
[2]National Institute for Research in Inorganic Materials, Namiki, Tsukuba, 305-0044
[3]Faculty of Engineering, Kanagawa University, Rokkakubashi, Kanagawa-ku, Yokohama 221-8686 Japan

(Received October 19; in revised form December 22, 1998)

Abstract

The heat capacity of 9.70 and 11.35 mol% yttria stabilized zirconia ($(ZrO_2)_{1-x}(Y_2O_3)_x$; x=0.0970, 0.1135) was measured by adiabatic calorimetry between 13 and 300 K, and some thermodynamic functions were calculated and given in a table. A large excess heat capacity extending from the lowest temperature to room temperature with a broad maximum at about 75 K was found in comparison with the heat capacity calculated from those of pure zirconia and yttria on the basis of simple additivity rule. The shape of the excess heat capacity is very similar to the Schottky anomaly, which may be attributed to a softening of lattice vibration. The amount of the excess heat capacity decreased with increasing yttria doping, while the maximum temperature did not vary. The relationships among the excess heat capacity, defect structure and interatomic force constants, and also the role of oxygen vacancy were discussed.

Keywords: heat capacity, oxygen defect, softening in lattice vibration, thermodynamic functions, yttria stabilized zirconia

Introduction

The structure of pure zirconia ZrO_2 is monoclinic at room temperature, and it undergoes monoclinic-tetragonal and tetragonal-cubic structural phase transitions at 1440 and 2670 K in the atmosphere, respectively. However, the fluorite type cubic structure of the high temperature phase can exist at room temperature by doping lower valent metal oxides (e.g. CaO, Y_2O_3, lanthanoid sesquioxides, etc.); that is so-called stabilized zirconia (YSZ). By incorporating the di- or tri-valent metal oxides, the oxygen vacancies are formed on the anion sublattice for charge compensation. The oxygen ions become mobile via the vacancies at high temperatures, and the sta-

* Author for correspondence: tel.: +81-45-924-5343, fax:+81-45-924-5339, e-mail: atake1@rlem.titech.ac.jp

1418–2874/99/ $ 5.00
© 1999 Akadémiai Kiadó, Budapest
Akadémiai Kiadó, Budapest
Kluwer Academic Publishers, Dordrecht

bilized zirconia is an excellent superionic conductor. In the region of low dopant concentrations, the conductivity increases with increasing dopant concentration. However, the conductivity exhibits a maximum at about 8 mol% in the case of yttria, and a further doping reduces the conductivity [1]. On the other hand, the activation energy of the electronic conductivity shows a minimum at the concentration and it increases by further doping. Such behaviour has been explained by vacancy-vacancy interaction [2], dopant-vacancy association [3, 4] and formation of microdomains [5], etc. Therefore, the information regarding the details of defect structure is important to elucidate the mechanisms for the oxygen conductivity.

The defect structure of stabilized zirconia has been studied extensively by means of X-ray [6, 7], electron [8] and neutron diffraction [9–11], and site selective spectroscopy [12]. Many authors have reported that the anions and cations are displaced from their ideal positions of the fluorite structure due to the oxygen vacancies, and the anion sublattice is distorted [8]. The EXAFS technique has been also employed to investigate the local structure [13–16], and the analysis of the data shows that the oxygen vacancies are sited in the first neighbors to Zr ion and Y ion is always in 8 coordination. A similarity has been also suggested of the local structure of 7 coordinated zirconium cations to those in monoclinic zirconia. By the stabilization of the cubic structure and the complex oxygen displacements, the cation-anion and anion-anion interactions should be significantly altered.

It is well known that the defects in the crystal induce some localized modes, and alter the vibrational density of states and thus the lattice heat capacity. The defect-induced modes should be related to the local defect structures, and they can be studied by heat capacity measurements. Recently, for the 7.76 mol% yttria stabilized zirconia, we have found an excess heat capacity extending from the lowest temperature to room temperature with a broad maximum at about 75 K, compared with the calculated heat capacity from those of pure zirconia and yttria based on the simple additivity rule [17]. It has been proposed that the excess heat capacity is caused by a softening in the lattice vibrations, which is ascribed to the formation of oxygen defects and/or the stabilization of the cubic structure. In the present study, we have extended the experiments to further doping samples; 9.70 and 11.35 mol% yttria stabilized zirconia. The results will be analyzed together with the previous results [17] from the viewpoint of lattice vibration. The relationship between the local defect structure and excess heat capacity will be discussed. Some thermodynamic functions calculated from the measured heat capacity values will be tabulated.

Experimental

The samples of 9.70 and 11.35 mol% yttria stabilized zirconia polycrystals were prepared by a hydrolysis method from a mixture of $ZrOCl_2 \cdot 8H_2O$ (Tosoh Co. Ltd., Japan) and YCl_3 (commercial grade) solutions. The product was spray-dried, followed by a treatment in steam flow for dechlorination. The powder obtained was calcined at 1120 K. The averaged particle size was estimated to be about 0.45 μm estimated by scanning electron microscope observations. The powder was pressed into

a plate uniaxially under 50, and then isostatically cold-pressed under 200 MPa. The green compact was sintered at 1770 K in air for 4 h. It has been established that the sintered sample which has reduced specific surface area is little influenced by surface adsorption effects [18]. A single phase of the cubic structure of the samples was confirmed by X-ray powder diffractometry at room temperature. The yttrium content of the samples were determined to be x=0.0970 and 0.1135 in $(ZrO_2)_{1-x}(Y_2O_3)_x$ by inductively coupled plasma spectrometry. The density of the sintered samples was 94, 91 per cent of the theoretical value for 9.70 and 11.35 mol% yttria stabilized zirconia, respectively.

Heat capacity measurements have been made by using a homemade adiabatic calorimeter [19, 20]. A working thermometer was a platinum resistance thermometer (type 5187L, H. Tinsley and Co., Ltd.), which is permanently mounted together with the calorimeter heater on the calorimeter vessel. The thermometer was calibrated at National Physical Laboratory (England) *vs*. the ITS-90 between 13 and 306 K. The calorimeter vessel, which is made of a gold-plated copper, has a mass of about 29.36 g including the thermometer and a calorimeter heater, etc. The sample used for the calorimetry was amounted to 18.7671 and 16.1482 g of 9.70 and 11.35 mol% yttria stabilized zirconia, respectively. The temperature increment by a single heat input for each measurement was about 1 in the lowest temperature region, and it increased to about 2 K at room temperature. The heat capacity of the sample at 50, 150 and 300 K amounted to 25, 38 and 45%, and 22, 34 and 42% of the total heat capacity (the sample and the calorimeter vessel) for 9.70 and 11.35 mol% yttria stabilized zirconia samples, respectively. No anomalous behavior, such as self-heating, supercool phenomena or discontinuity of heat capacity, was observed during the experiments.

Results and discussion

The heat capacity of 9.70 and 11.35 mol% yttria stabilized zirconia $\{(ZrO_2)_{1-x}(Y_2O_3)_x$; x=0.0970, 0.1135$\}$ has been measured by adiabatic calorimetry between 13 and 300 K. The primary data of the molar heat capacity of 9.70 and 11.35 mol% yttria stabilized zirconia without curvature corrections are given in Tables 1 and 2, respectively. The smoothed heat capacity curve was calculated using a method of least square fitting; the data were divided into several temperature regions and then fitted by polynomial expressions. The heat capacity below 13 K was estimated by a graphical smooth extrapolation. The standard molar thermodynamic functions derived from the smoothed heat capacity values at rounded temperatures are given in Tables 3 and 4.

The molar heat capacities of 9.70 and 11.35 mol% yttria stabilized zirconia are plotted as a function of temperature in Fig. 1, together with the previous results of pure zirconia and 7.76 mol% yttria stabilized zirconia [17]. It looks apparently that the yttria stabilized zirconia of higher yttria doping has larger heat capacity. However, in the lowest temperature region, the sample of 11.35 mol% yttria doped zirconia has the smallest value of heat capacity as seen in Fig. 2; the crossing over occurs at about 60 K. As the vibrational motions should be highly excited in the higher

Table 1 Molar heat capacity of $(ZrO_2)_{0.9030}(Y_2O_3)_{0.0970}$ (M=133.169 g mol^{-1})

T/ K	$C_{p,m}$/ J $K^{-1}mol^{-1}$	T/ K	$C_{p,m}$/ J $K^{-1}mol^{-1}$	T/ K	$C_{p,m}$/ J $K^{-1}mol^{-1}$	T/ K	$C_{p,m}$/ J $K^{-1}mol^{-1}$	T/ K	$C_{p,m}$/ J $K^{-1}mol^{-1}$
(Series 1)		61.988	10.264	122.80	28.646	185.99	44.169	252.07	55.466
14.647	0.2058	63.886	10.840	124.85	29.269	188.20	44.647	254.20	55.771
15.647	0.2600	65.738	11.406	126.94	29.803	190.42	45.082	256.31	56.046
16.720	0.3252	67.626	11.982	129.08	30.397	192.66	45.538	258.42	56.331
17.894	0.4050	69.584	12.585	131.19	30.983	194.91	45.992	260.52	56.594
19.140	0.5015	71.546	13.186	133.28	31.546	197.15	46.414	262.61	56.864
20.405	0.6140	73.478	13.782	135.41	32.125	199.37	46.831	264.70	57.127
21.705	0.7437	75.447	14.392	137.58	32.724	201.61	47.285	266.80	57.389
23.102	0.9036	77.454	15.016	139.73	33.279	203.86	47.709	268.96	57.672
24.576	1.0890	79.417	15.630	141.87	33.834	206.10	48.112	271.14	57.948
26.058	1.2974	81.342	16.223	144.02	34.413	208.33	48.516	273.34	58.233
27.569	1.5254	83.253	16.812	146.15	34.945	210.54	48.922	275.57	58.460
29.167	1.7948	85.175	17.405	148.28	35.507	212.74	49.293	277.79	58.715
30.803	2.0890	87.140	18.019	150.46	36.051	214.96	49.711	279.99	59.019
32.465	2.4116	89.171	18.647	152.67	36.592	217.19	50.145	282.19	59.272
34.181	2.7607	91.240	19.280	154.86	37.140	219.41	50.461	284.39	59.563
35.963	3.1473	93.326	19.920	157.02	37.674	221.62	50.821	286.58	59.768
37.767	3.5567	95.389	20.550	159.17	38.198	223.82	51.211	288.78	60.008
39.570	3.9877	97.449	21.181	161.30	38.690	226.01	51.578	291.02	60.278
41.391	4.4369	99.511	21.801	163.41	39.206	228.19	51.911	293.24	60.492
43.183	4.9003	101.58	22.427	165.51	39.705	230.36	52.259	295.46	60.727
45.011	5.3801	103.67	23.055	167.59	40.181	232.55	52.598	297.67	60.971
46.905	5.8865	105.81	23.691	169.65	40.625	234.76	52.928	299.88	61.207
48.830	6.4207	107.97	24.342	171.69	41.092	236.96	53.247		
50.727	6.9565	110.09	24.963	173.73	41.548	239.14	53.605		
52.579	7.4843	112.18	25.572	175.74	41.981	241.32	53.941		
54.434	8.0193	114.31	26.198	177.75	42.430	243.49	54.257		
56.322	8.5706	116.48	26.832	179.74	42.849	245.65	54.559		
58.214	9.1337	118.62	27.435	181.76	43.299	247.80	54.861		
60.094	9.6971	120.72	28.044	183.84	43.717	249.94	55.185		

Table 2 Molar heat capacity of $(ZrO_2)_{0.8865}(Y_2O_3)_{0.1135}$ (M=134.867 g mol^{-1})

T/ K	$C_{p,m}$/ J $K^{-1}mol^{-1}$	T/ K	$C_{p,m}$/ J $K^{-1}mol^{-1}$	T/ K	$C_{p,m}$/ J $K^{-1}mol^{-1}$	T/ K	$C_{p,m}$/ J $K^{-1}mol^{-1}$	T/ K	$C_{p,m}$/ J $K^{-1}mol^{-1}$
(Series 1)		78.647	15.363	153.20	37.070	239.34	54.205	231.1	52.930
13.968	0.1583	80.507	15.946	155.30	37.600	241.55	54.517	233.29	53.251
15.057	0.2098	82.390	16.536	157.42	38.125	243.75	54.852	235.47	53.559
16.227	0.2721	84.282	17.129	159.54	38.637	245.95	55.116	237.66	53.927
17.485	0.3496	86.166	17.716	161.64	39.154	248.13	55.513	239.88	54.254
18.803	0.4423	88.005	18.293	163.72	39.656	250.31	55.806	242.09	54.564
20.179	0.5556	89.802	18.852	165.84	40.161	252.48	56.092	244.28	54.950
21.624	0.6934	91.669	19.445	168.02	40.670	254.67	56.377	246.47	55.242
23.106	0.8548	93.624	20.057	170.20	41.164	256.88	56.702	248.65	55.503
24.489	1.0228	95.579	20.661	172.39	41.678	259.08	56.972	250.85	55.881
25.835	1.2034	97.536	21.267	174.59	42.176	261.27	57.248	253.07	56.178
27.343	1.4278	99.476	21.859	176.78	42.642	263.46	57.605	255.28	56.430
28.853	1.6702	101.47	22.480	178.94	43.107	265.64	57.825	257.49	56.793
30.326	1.9258	103.50	23.097	181.10	43.587	267.84	58.131	259.68	57.063
31.895	2.2186	105.51	23.705	183.26	44.050	270.06	58.403	261.87	57.328
33.559	2.5470	107.47	24.300	185.44	44.508	272.28	58.671	264.05	57.666
35.185	2.8902	109.41	24.885	187.63	44.965	274.48	58.893	266.22	57.916
36.901	3.2698	111.32	25.462	189.86	45.435	276.68	59.185	268.38	58.195
38.760	3.7004	113.19	26.016	192.10	45.890	278.88	59.456	270.54	58.431
40.561	4.1368	115.04	26.565	194.33	46.348	281.07	59.675	272.69	58.729
42.354	4.5888	116.87	27.105	196.54	46.781	283.24	59.977	274.83	58.967
44.155	5.0556	118.67	27.631	198.75	47.222	285.42	60.231	276.99	59.225
46.005	5.5492	120.45	28.151	200.93	47.657	287.58	60.421	279.18	59.510
47.897	6.0659	122.21	28.667	203.11	48.049	289.74	60.767	281.39	59.757
49.744	6.5812	123.95	29.194	205.27	48.462	291.89	60.962	283.62	60.028
51.575	7.0995	125.67	29.652	207.43	48.848	294.03	61.179	285.85	60.290
53.448	7.6393	127.38	30.135	209.57	49.255	296.18	61.347	288.06	60.529
55.344	8.1935	129.06	30.607	211.70	49.637	298.31	61.648	290.27	60.814
57.255	8.7619	130.73	31.079	213.81	50.018	300.43	61.866	292.47	60.987
59.171	9.3340	132.39	31.517	215.92	50.368	(Series 2)		294.67	61.239
61.027	9.8944	134.02	31.994	218.02	50.803	209.34	49.209	296.86	61.484
62.801	10.432	135.65	32.441	220.11	51.114	211.52	49.605	299.05	61.705
64.501	10.963	137.26	32.879	222.19	51.462	213.69	49.995		
66.238	11.489	138.85	33.308	224.26	51.830	215.85	50.357		

Table 2 Continued

T/ K	$C_{p,m}$/ J K^{-1}mol^{-1}	T/ K	$C_{p,m}$/ J K^{-1}mol^{-1}	T/ K	$C_{p,m}$/ J K^{-1}mol^{-1}	T/ K	$C_{p,m}$/ J K^{-1}mol^{-1}	T/ K	$C_{p,m}$/ J K^{-1}mol^{-1}
68.044	12.048	140.63	33.795	226.34	52.150	217.99	50.795		
69.850	12.607	142.64	34.333	228.47	52.487	220.16	51.116		
71.628	13.159	144.73	34.888	230.62	52.861	222.34	51.436		
73.400	13.711	146.87	35.448	232.79	53.190	224.51	51.844		
75.169	14.267	148.99	35.996	234.97	53.527	226.70	52.190		
76.886	14.805	151.09	36.532	237.15	53.805	228.91	52.527		

temperature region, the heat capacity value becomes to the classical limiting value with increasing temperature, which should be proportional to the degrees of freedom, that is the number of atoms in the chemical formula. Therefore, at high tem-

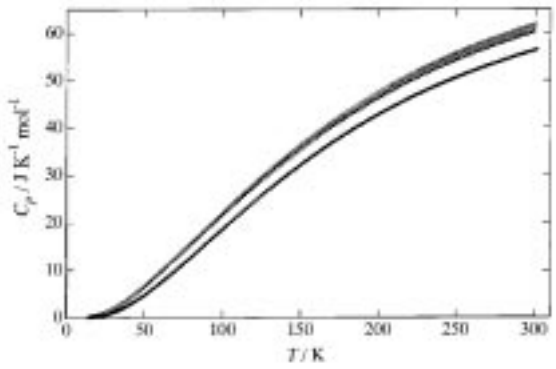

Fig. 1 Molar heat capacity of pure zirconia and yttria stabilized zirconia. • – Pure zirconia [17]; ▲ – 7.76 mol% YSZ [17]; △ – 9.70 mol% YSZ; ◊ –11.35 mol% YSZ

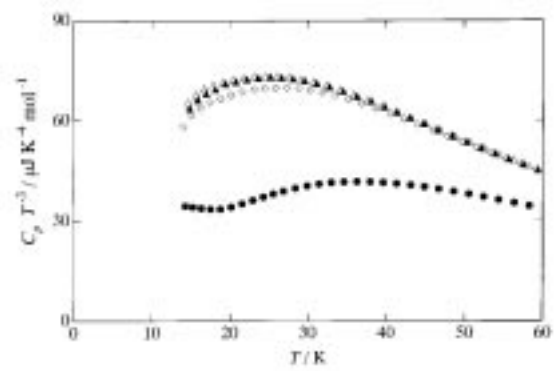

Fig. 2 Molar heat capacity of pure zirconia and yttria stabilized zirconia plotted as C_pT^{-3} *vs.* *T*. • – Pure zirconia [17]; ▲– 7.76 mol% YSZ [17]; △ – 9.70 mol% YSZ; ◊ – 11.35 mol% YSZ

peratures the yttria stabilized zirconia of high yttria doping has larger heat capacity because the number of atoms in the chemical formula $(ZrO_2)_{1-x}(Y_2O_3)_x$ increases with increasing the value of x. On the other hand, the heat capacity should depend not only on the degrees of freedom but also on the force constants at low temperatures where the vibrational motion is not highly excited; classical thermodynamics should not be applicable, but quantum mechanical effects should be considered. In Fig. 2, the yttria stabilized zirconia shows much larger heat capacity than pure zirconia, which is due to so-called low-lying modes. It should be noted that the ionic conductivity at elevated temperatures shows also a maximum at about the composition of 8–10 mol% of yttria doping.

In order to analyze the effect of yttria doping quantitatively, the heat capacity of yttria stabilized zirconia was calculated from the heat capacity of pure zirconia and yttria based on the simple additivity rule; $(1-x)C_p^{ZrO_2} + xC_p^{Y_2O_3}$, where $C_p^{ZO_2}$ and $C_p^{Y_2O_3}$ are the heat capacity of pure zirconia [17] and yttria [21], respectively. The difference between the experimental (C_p^{YSZ}) and the calculated heat capacity of yttria stabilized zirconia is given as:

$$\Delta C_p = C_p^{YSZ} - [(1-x)C_p^{ZrO_2} + xC_p^{Y_2O_3}] \quad (1)$$

The results of the calculation for 7.76, 9.70 and 11.35 mol% yttria stabilized zirconia are shown in Fig. 3, where large excess heat capacity is seen clearly extending from the lowest temperature to room temperature with a broad maximum at about 75 K. The shape of the excess heat capacity is very similar to a typical Schottky anomaly [22]. In the previous paper [17], it has been reported that the such anomaly is supposed to be a result of a kind of softening in lattice vibrations, which may be due to the formation of oxygen vacancy and/or the structural modification from monoclinic to cubic structure by the yttria doping. In Fig. 3(a), the excess heat capacity decreases with increasing the dopant concentration. Figure 3(b) shows a scaled plot of the excess heat capacity by the factor of a derived from their peak heights. It should be noted that the shapes of the excess heat capacities are extremely similar to each other and the maximum temperature is not influenced by the composition. According to the explanation on the basis of the softening in lattice vibration [17], such behaviour implies that the softening modes vanish gradually with proceeding yttria doping, and the vibrational density of states of yttria stabilized zirconia may become that of simple additivity rule.

There are two possible mechanisms for the softening, which brings about the excess heat capacity. One is the impurity modes induced by the substituting yttrium ions or oxygen vacancies, that is different from the normal vibrations in pure zirconia. The other is the difference between the atomic arrangements of the monoclinic and cubic structure, in which the atomic interactions and lattice vibrations are different. In the former case, the excess heat capacity at low temperatures should increase with increasing yttria doping. In fact, however, it shows a maximum at about 8 mol% doping, and we must assume another effect such as clustering of the vacancies for further doping. In the latter case, the excess heat capacity deduced from the simple additivity rule decreases monotonously with increasing yttria doping. In the

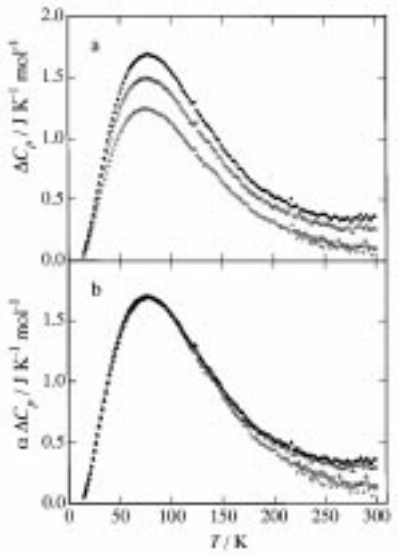

Fig. 3 Excess heat capacity derived from the assumption of simple additivity rule. $\Delta C_p = C_p^{YSZ} - [(1-x)C_p^{ZrO_2} + xC_p^{Y_2O_3}]$. ▲– 7.76 mol% YSZ [17]; ▵ – 9.70 mol% YSZ; ◊ – 11.35 mol% YSZ (a). Excess heat capacity scaled with a factor of α . ▲ – 7.76mo1% YSZ (α=1.00) [17]; ▵ – 9.70 mol% YSZ (α=1.13); ◊ – 11.35 mol% YSZ (α=1.36) (b)

cubic fluorite structure, zirconium ion should be in the site of 8 coordination with oxygen ions, while in the monoclinic distorted structure of pure zirconia zirconium ion is surrounded by 7 nearest neighbor anions. The local structural studies by EXAFS [14–16] have reported that an oxygen vacancy is rather sited in the nearest neighbor position of a zirconium ion, not in that of the trivalent yttrium ion expected from the local charge compensation, and the mean coordination number of the zirconium ion is reduced to 7. It has been also pointed out the similarity of the local environment, such as coordination number and Zr–O interatomic distance, of the 7 fold coordinated zirconium ion in the cubic stabilized zirconia to that in pure monoclinic zirconia. The vibrational analysis on the Debye-Waller factors showed also the similarity of the frequency of the Zr–O vibration in the stabilized zirconia to that pure monoclinic zirconia [23]. Because the number of the vacancies is limited, a large number of zirconium ions still remain in 8 coordination at low dopant concentrations. With increasing yttria content, the number of 8 coordinated zirconium ions decreases and the sites are replaced by the 7 coordinated zirconium ions. Therefore the softened modes are attributed to the vibrations of the 8 coordinated zirconium ions and its surrounding anions. This well explains the behaviour of the excess heat capacity obtained in the present experiments. The amount of the excess heat capacity is proportional to the number of the 8 coordinated zirconium ions, which either decrease with increasing yttria content. The good coincidence among the shapes of the excess heat capacities shown in Fig. 3(b) implies the softening modes decrease with increasing yttria content and the modes similar to the normal vibrations in pure

Table 3 Thermodynamic functions of $(ZrO_2)_{0.9030}(Y_2O_3)_{0.0970}$ (M=133.169 g mol^{-1}) $\Phi^o_m = \Delta^T_0 S^o_m - \Delta^T_0 H^o_m/T$. The entropy value is assumed to be 0 at 0 K

T/ K	$C^o_{p,m}$/ J K^{-1}mol^{-1}	$\Delta^T_0 H^o_m$/ J mol^{-1}	$\Delta^T_0 S^o_m$/ J K^{-1}mol^{-1}	Φ^o_m/ J K^{-1}mol^{-1}
15	0.224	0.740	0.0633	0.0140
20	0.5761	2.664	0.1716	0.03839
30	1.942	14.51	0.6333	0.1497
40	4.092	44.14	1.471	0.3675
50	6.749	98.05	2.663	0.7019
60	9.667	180.0	4.148	1.149
70	12.71	291.8	5.866	1.698
80	15.81	434.4	7.765	2.336
90	18.90	607.9	9.806	3.051
100	21.95	812.2	11.96	3.833
110	24.94	1047	14.19	4.673
120	27.84	1311	16.48	5.561
130	30.65	1603	18.82	6.491
140	33.35	1923	21.19	7.456
150	35.94	2270	23.58	8.452
160	38.39	2642	25.98	9.472
170	40.71	3037	28.38	10.51
180	42.91	3455	30.77	11.57
190	45.00	3895	33.15	12.65
200	46.97	4355	35.51	13.73
210	48.82	4834	37.84	14.82
220	50.56	5331	40.15	15.92
230	52.20	5845	42.44	17.03
240	53.74	6375	44.69	18.13
250	55.18	6919	46.92	19.24
260	56.53	7478	49.11	20.34
270	57.80	8050	51.26	21.45
280	59.01	8634	53.39	22.55
290	60.15	9230	55.48	23.65
298.15	61.02	9723	57.16	24.55
300	61.22	9837	57.54	24.75

Table 4 Thermodyanmic functions of $(ZrO_2)_{0.8865}(Y_2O_3)_{0.1135}$ (M=134.867 g mol^{-1}) $\Phi_m^o = \Delta_0^T S_m^o - \Delta_0^T H_m^o / T$. The entropy value is assumed to be 0 at 0 K

T/ K	$C_{p,m}^o$/ J K^{-1}mol^{-1}	$\Delta_0^T H_m^o$/ J mol^{-1}	$\Delta_0^T S_m^o$/ J K^{-1}mol^{-1}	Φ_m^o/ J K^{-1}mol^{-1}
15	0.207	0.652	0.0551	0.0116
20	0.5400	2.441	0.1557	0.03367
30	1.868	13.72	0.5952	0.1377
40	3.999	42.50	1.408	0.3459
50	6.652	95.45	2.579	0.6699
60	9.584	176.5	4.048	1.107
70	12.65	287.6	5.755	1.646
80	15.78	429.7	7.648	2.277
90	18.92	603.3	9.689	2.986
100	22.02	808.0	11.84	3.763
110	25.06	1044	14.09	4.599
120	28.02	1309	16.39	5.485
130	30.87	1604	18.75	6.415
140	33.62	1926	21.14	7.381
150	36.26	2276	23.55	8.378
160	38.76	2651	25.97	9.402
170	41.12	3050	28.39	10.45
180	43.35	3473	30.81	11.51
190	45.46	3917	33.21	12.59
200	47.46	4382	35.59	13.68
210	49.33	4866	37.95	14.78
220	51.09	5368	40.29	15.89
230	52.73	5887	42.59	17.00
240	54.28	6422	44.87	18.11
250	55.74	6972	47.12	19.23
260	57.11	7537	49.33	20.34
270	58.38	8114	51.51	21.46
280	59.59	8704	53.66	22.57
290	60.74	9306	55.77	23.68
298.15	61.62	9805	57.46	24.58
300	61.81	9919	57.84	24.78

monoclinic zirconia increases simultaneously. Thus the similarity of the vibrations related to the 7 coordinated zirconium ions of cubic stabilized zirconia to that of pure monoclinic zirconia is suggested. The details of the phonon dispersion relations of the stabilized zirconia are not fully clarified by the neutron studies because of the static disorders in the oxygen sublattice [24, 25]. The heat capacity measured in the present study apparently shows the drastic changes in the lattice vibrations. It is also suggested from the relative difference in the vibrational frequencies that the 7 coordinated zirconium ions are more tightly bonded to oxygen ions than the 8 coordinated zirconium ions. Such difference in atomic interactions may be reflected on the ionic conductivity, especially on the process of the exchanging oxygen and vacancy at high temperatures. The relationship between the activation energy of the electric conduction and the defect structure should be clarified by further studies.

Conclusions

The heat capacity of 9.70 and 11.35 mol% yttria stabilized zirconia has been measured by adiabatic calorimetry between 13 and 300 K, and the results were analyzed together with the previous results on 7.76 mol% yttria stabilized zirconia and pure zirconia. The excess heat capacity was found in comparison with the value calculated on the basis of simple additivity rule. The excess heat capacity is attributed to the stabilization of the cubic structure by the yttria doping. The softening modes induced may be corresponded to the vibrations of 8 coordinated zirconium ion and surrounding oxygen ions. However, such softening is reduced by increasing the number of vacancies because the local atomic arrangement of the 7 coordinated zirconium ion in cubic stabilized zirconia may similar to that in the pure monoclinic zirconia. The oxygen vacancies play an important role in the mechanism.

References

1 D. W. Strickler and W. G. Carlson, J. Am. Ceram. Soc., 47 (1964) 122.
2 H. Schmalzried, Z. Physik. Chem. Neue Folge, 105 (1977) 47.
3 W. C. Mackrodt and P. M. Woodrow, J. Am. Ceram. Soc., 69 (1986) 277.
4 C. R. A. Catlow, Solid State Ionics, 12 (1984) 67.
5 J. G. Allpress and H. J. Rossell, J. Solid State Chem., 15 (1975) 68.
6 T. R. Welberry, B. D. Butler, J. G. Thompson and R. L. Withers, J. Solid State Chem., 106 (1993) 461.
7 M. Morinaga, J. B. Cohen and J. Faber, Jr., Acta Cryst., A36 (1980) 520.
8 K. J. McClellan, S.-Q. Xiao, K. P. D. Lagerlof and A. H. Heuer, Philos. Mag. A, 70 (1994) 185.
9 D. N. Argyriou, M. M. Elcombe and A. C. Larson, J. Phys. Chem. Solids, 57 (1996) 183.
10 J. Faber, Jr., M. H. Mueller and B. R. Cooper, Phys. Rev. B, 17 (1978) 4884.
11 D. Steele and B. E. F. Fender, J. Phys. C: Solid State Phys., 7 (1974) 1.
12 J. Dexpert-Ghys, M. Faucher and P. Caro, J. Solid State Chem., 54 (1984) 179.
13 P. Li, I.-W. Chen and J. E. Penner-Hahn, Phys. Rev. B, 48 (1993) 10063.
14 P. Li, I.-W. Chen and J. E. Penner-Hahn, Phys. Rev. B, 48 (1993) 10074.
15 P. Li, I.-W. Chen and J. E. Penner-Hahn, J. Am. Ceram. Soc., 77 (1994) 118.

16 C. R. A. Catlow, A. V. Chadwick, G. N. Greaves and L. M. Moroney, J. Am. Ceram. Soc., 69 (1986) 272.
17 T. Tojo, T. Atake, T. Mori and H. Yamamura, submitted to J. Chem. Thermodynamics.
18 T. Tojo, T. Atake, T. Shirakami, T. Mori and H. Yamamura, Solid State Ionics, 86-88 (1996) 89.
19 T. Atake, H. Kawaji, A. Hamano and Y. Saito, Rep. Res. Lab. Eng. Mater., Tokyo Inst. Tech., 15 (1990) 13.
20 T. Tanaka, T. Atake, H. Nakayama, T. Eguchi, K. Saito and I. Ikemoto, J. Chem. Thermodynamics, 26 (1994) 1231.
21 K. S. Gavrichev, V. E. Gorbunov, L. N. Golushina, G. E. Nikiforova, G. A. Totrova and J. S. Shaplygin, Russ. J. Phys. Chem., 67 (1993) 1554.
22 E. S. R. Gopal, Specific Heats at Low Temperatures, Plenum Press: New York 1962, p. 102.
23 P. Li, I.-W. Chen and J. E. Penner-Hahn, Phys. Rev. B, 48 (1993) 10082.
24 D. W. Liu, C. H. Perry, A. A. Feinberg and R. Currat, Phys. Rev. B, 36 (1987) 9212.
25 D. N. Argyriou and M. M. Elcombe, J. Phys. Chem. Solids, 57 (1996) 343.